Versão do arquivo anexado / Version of attached file:

Versão do Editor / Published Version

Mais informações no site da editora / Further information on publisher's website:

https://www.sciencedirect.com/science/article/pii/S0375947418301957

DOI: 10.1016/j.nuclphysa.2018.09.007

Direitos autorais / Publisher's copyright statement:

XXVIIth International Conference on Ultrarelativistic Nucleus-Nucleus Collisions
(Quark Matter 2018)

Exploring the Phase Space of Jet Splittings at ALICE using Grooming and Recursive Techniques

Harry Arthur Andrews
on behalf of the ALICE collaboration

University of Birmingham

Abstract

Hard splittings in the evolution of a hard scattered parton may be modified by the presence of a dense strongly interacting medium. Grooming procedures can be used to isolate such hard components of a jet and allows one to focus on the two subjets resulting from a sufficiently hard partonic splitting. Measurements of the symmetry parameter (z_g), angular separation (R_g) and number of splittings (n_{SD}) of Soft Drop groomed jets are reported as measured with the ALICE Detector in pp and Pb–Pb collisions at $\sqrt{s}$= 7 TeV and $\sqrt{s_{NN}}$= 2.76 TeV, respectively. The use of recursive splittings and their mappings to identify interesting regions of phase space in the $z_g - Rg$ plane are also discussed.

1. Introduction

1.1. Jet Grooming

In relativistic heavy ion collisions, exchanges of large momentum between partonic constituents occur in the early stages and, subsequently, the scattered partons traverse the hot and dense medium of deconfined colour charges. Partons that evolve in the presence of this medium are known to experience energy loss, commonly referred to as jet quenching [1]. This energy loss is thought to occur dominantly due to gluon radiation induced by the medium [2][3]. Understanding how the fragmentation pattern of jets is modified by the medium is the main scope of this analysis. The soft components of these modifications are very difficult to measure and model. However, studying the limit of the hardest components of the parton shower, that can occur in the jet cone, can provide information on how these medium-induced processes take place. In addition to studying medium-induced fragmentation, investigating the properties of the the hard components of the parton shower can help to elucidate the role of coherent and decoherent emissions in the presence of the coloured medium [4].

In order to study these leading components of the parton shower, jets are groomed to identify hard splittings using the Soft Drop jet grooming algorithm [5][6]. Soft Drop begins the grooming procedure by first reclustering the jet constituents with a given algorithm, most commonly Cambridge-Aachen (CA) [7], and unwinding the clustering one step. The resulting pairs of subjets are then considered and the sub-leading

subjet momentum fraction, z, is calculated as $z = \frac{min(p_{T,1}, p_{T,2})}{p_{T,1}+p_{T,2}}$, where $p_{T,1}$ and $p_{T,2}$ are the transverse momenta of the two subjets. If this momentum fraction satisfies the grooming condition:

$$z > z_{\text{cut}} \left(\frac{\Delta R}{R_0} \right)^{\beta},\qquad(1)$$

where z_{cut} and β are grooming variables set by the user, ΔR is the angular separation of the two subjets and R_0 is the jet radius, the splitting identified is considered sufficiently hard and the grooming procedure is stopped. If the condition is not satisfied then the softer subjet is discarded and the clustering of the harder branch is unwound an additional step; this process is repeated until a splitting satisfying (1) is found. The momentum fraction at this stage is identified as the groomed momentum fraction z_g. The angular separation of the two subjets, as defined in the $\eta - \varphi$ plane, is another important parameter of the splitting and is assigned as the groomed radius $R_g = \sqrt{(\eta_{\text{subjet,1}} - \eta_{\text{subjet,2}})^2 + (\varphi_{\text{subjet,1}} - \varphi_{\text{subjet,2}})^2}$. Reclustering with the CA algorithm is designed to replicate the angular ordering of QCD vacuum splittings and, to leading order, the z_g spectrum in vacuum is very close to the Altarelli-Parisi splitting functions.

In addition to studying the parameters of the leading hard splitting of jets the number of them that arise in the evolution of the jet can help identify any additional splittings occurring due to the presence of the medium. To count the total number of splittings, the grooming is continued past the first splitting to satisfy (1) and, following the hardest branch at each stage, the total number that pass the condition are counted and assigned as n_{SD}.

1.2. The Lund Plane

A very useful representation of the splittings is the Lund kinematical diagram. The Lund diagram represents the $1 \to 2$ splitting process of a parton on the two axes as shown in Fig.1. The axes reflect the gluon emission probability given by $dP = 2\frac{\alpha_s C_i}{\pi} \text{dlog}(z\theta)\text{dlog}\frac{1}{\theta}$, where θ is the aperture angle of the splitting, z is the momentum fraction of the two outgoing partons and C_i is the colour factor for a gluon radiated off an initial quark ($C_i = C_F$) or gluon ($C_i = N_c$).

Representing the phase space of splittings in this way allows one to isolate regions where different medium-induced mechanisms are expected to contribute to the modification of the parton shower splitting function. As it can be seen in Fig. 1 (left) the region where soft wide angle splittings dominate can be clearly separated from the region of hard collinear splittings. Fig. 1 (right) shows how this diagram is populated with recursive splittings generated using PYTHIA 6.4 Perugia Tune 2011 [8] and identified using CA reclustering.
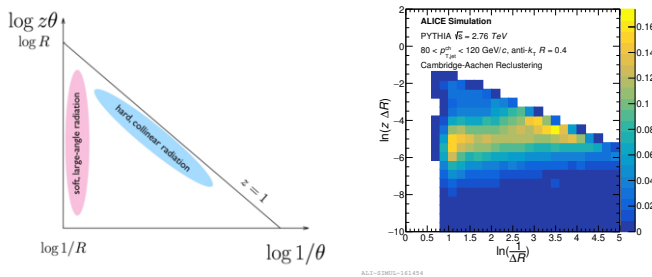

Fig. 1: Lund kinematical diagram representation of splittings with limits imposed by a jet resolution R (left) [9], and populated for splittings in vacuum PYTHIA 6.4 Perugia 11 (right).

2. Analysis Procedure

In this analysis, results from pp at $\sqrt{s}$= 7 TeV and Pb–Pb collisions at $\sqrt{s_{\text{NN}}}$= 2.76 TeV recorderd by the ALICE detector are presented. Charged jets were reconstructed with a minimum track transverse

momentum of $p_{\mathrm{T,track}}^{\mathrm{ch}} > 150$ MeV/c and clustered using the FastJet anti-k_{T} algorithm [10] with a resolution parameter $R = 0.4$ [11]. The jet track candidates were combined using the E-scheme prescription. In the pp measurements, there was no background subtraction applied to the jet and in the Pb–Pb analysis constituent subtraction [12] was used to remove the uncorrelated underlying event.

3. Results

The spectra of z_{g}, R_{g} and n_{SD} in minimum bias pp collisions were corrected using a 2D-Bayesian unfolding approach to correct for detector effects. The detector effects were studied using GEANT3 on simulated PYTHIA jet events. The results for the pp collisions are presented in the range $40 \leq p_{\mathrm{T,jet}}^{\mathrm{ch}} < 60$ GeV/c [13]. Due to a lack of pp statistics at the Pb–Pb collision energy of $\sqrt{s_{\mathrm{NN}}} = 2.76$ TeV and the good agreement observed between pp data and PYTHIA at $\sqrt{s} = 7$ TeV, PYTHIA events at $\sqrt{s} = 2.76$ TeV were used as the vacuum reference for the Pb–Pb data.

In Pb–Pb collisions the measurements of z_{g} and n_{SD} were made in the range $80 \leq p_{\mathrm{T,jet}}^{\mathrm{ch,rec}} < 120$ GeV/c to avoid contamination from combinatorial background and compared to a smeared reference generated by embedding PYTHIA jets into 0-10% central Pb–Pb events. The spectra are uncorrected due to instabilities in the unfolding procedure. The measurement of z_{g} is studied differentially in R_{g}. As shown in Fig. 2, the R_{g} selection has a significant effect on the z_{g} distribution. For splittings at large angles (right) a steepening of the distribution is observed as well as an overall suppression in the number of jets selected by the grooming procedure above this threshold. Conversely in the collinear limit (left) no such modification is observed and the ratio of jets selected in this region is consistent between the Pb–Pb data and the vacuum reference. It is important to note that the distributions are normalised by the total number of jets in the given transverse momentum bin. This means that the integral of the distributions in the range $0.1 \leq z_{\mathrm{g}} < 0.5$ is not constant between the distributions and the bin labelled "unselected" shows the fraction of jets that do not enter this part of the distribution due to either the grooming conditions or cuts on R_{g}. This normalisation choice allows one to correctly attribute any modification of the distribution to a suppression or enhancement.
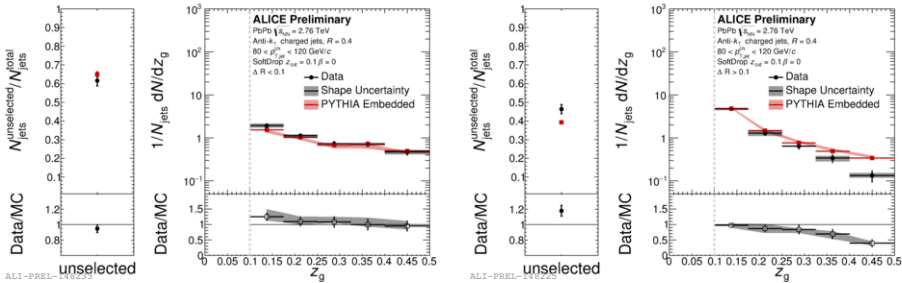

Fig. 2: Raw Pb–Pb distributions of z_{g} for $R = 0.4$ jets with varying minimum angular separation of subjets (R_{g}) for jets with $80 \leq p_{\mathrm{T,jet}}^{\mathrm{ch,rec}} < 120$ GeV/c. The distributions are normalised to the total number of jets in the sample in this $p_{\mathrm{T,jet}}^{\mathrm{ch,rec}}$ bin without cuts on R_{g}.

The measurement of n_{SD} which corresponds to the number of branches in the jet clustering history that satisfy the Soft Drop cut is shown in Fig. 3. This distribution shows no significant modification in the Pb–Pb data relative to vacuum data in the range $1 \leq n_{\mathrm{SD}} \leq 7$ with an enhancement observed in the "untagged" bin of $n_{\mathrm{SD}} = 0$.

Complimentary to the study of z_{g} differentially in R_{g}, the jet populations in the Lund plane can be used to identify regions of significant enhancement or suppression of jet production due to the presence of the medium. Fig. 4 shows the Lund plane for the difference between the first splitting of jets in data and embedded PYTHIA. Using this representation of the phase space purely as a pictorial representation it is shown that in the collinear limit there is a general region of very slight enhancement whereas in the large angle limit there is an overall depletion in data.
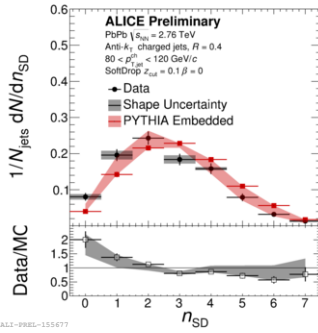
Fig. 3: Number of Soft Drop branches in the PbPb data jets and in PYTHIA embedded jets.
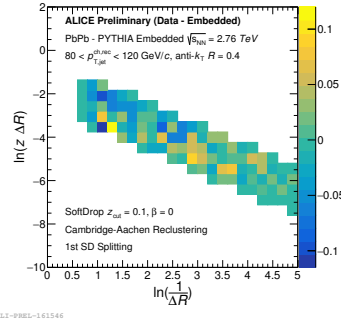

Fig. 4: Lund plane representing the difference between the first splitting identified in data and embedded PYTHIA.

4. Conclusions and Outlook

Measurements of z_g and n_{SD} have been reported in pp at $\sqrt{s} = 7$ TeV and Pb–Pb collisions at $\sqrt{s_{NN}} = 2.76$ TeV. A good agreement between pp collisions and PYTHIA is observed and PYTHIA events generated at $\sqrt{s} = 2.76$ TeV are used as a vacuum reference for comparison to Pb–Pb collisions. In Pb–Pb collisions, a significant modification of the z_g distribution is observed at large angles whilst in the collinear limit the Pb–Pb distribution of z_g is consistent with the PYTHIA reference. The modification in the large angle limit is attributed to a suppression of the symmetric splittings by normalising the distributions to the total number of jets in the jet transverse momentum range. The number of splittings, n_{SD}, is unmodified in Pb–Pb collisions. This suggests that the modification of the z_g distribution isn't driven by an enhancement of splittings in any particular region of phase space.

References

[1] N. Armesto, B. Cole, C. Gale, W. A. Horowitz, P. Jacobs, et al., Comparison of Jet Quenching Formalisms for a Quark-Gluon Plasma 'Brick', Phys.Rev. C86 (2012) 064904. arXiv:1106.1106, doi:10.1103/PhysRevC.86.064904.
[2] R.Baier, Yu.L.Dokshitzer, S. Peign, D. Schiff, Induced Gluon Radiation in a QCD Medium, Phys. Lett. B345 (1994) 277–286. arXiv:hep-ph/9411409v2, doi:10.1016/0370-2693(94)01617-L.
[3] M. Gyulassy, M. Plumer, Jet quenching in dense matter, Phys. Lett. B243 (1990) 432.
[4] Y. Mehtar-Tani, K. Tywoniuk, Groomed jets in heavy-ion collisions: sensitivity to medium-induced bremsstrahlung, JHEP 04 (2017) 125. arXiv:1610.08930, doi:10.1007/JHEP04(2017)125.
[5] M. Dasgupta, A. Fregoso, S. Marzani, G. P. Salam, Towards an understanding of jet substructure, JHEP 09 (2013) 029. arXiv:1307.0007, doi:10.1007/JHEP09(2013)029.
[6] A. J. Larkoski, S. Marzani, G. Soyez, J. Thaler, Soft Drop, JHEP 05 (2014) 146. arXiv:1402.2657, doi:10.1007/JHEP05(2014)146.
[7] Yu.L.Dokshitzer, G.D.Leder, S.Moretti, B.R.Webber, Better Jet Clustering Algorithms, JHEP 08 (1997) 001. arXiv:9707323, doi:10.1088/1126-6708/1997/08/001.
[8] T. Sjostrand, S. Mrenna, P. Z. Skands, PYTHIA 6.4 Physics and Manual, JHEP 05 (2006) 026. arXiv:hep-ph/0603175, doi:10.1088/1126-6708/2006/05/026.
[9] K. Tywoniuk, et al., CERN TH Institute "Novel tools and observables for jet physics in heavy-ion collisions"/5th Heavy Ion Jet Workshop (2017).
     URL https://indico.cern.ch/event/625585/
[10] M. Cacciari, G. P. Salam, G. Soyez, The anti-k_t jet clustering algorithm, JHEP 04 (2008) 063. arXiv:0802.1189, doi:10.1088/1126-6708/2008/04/063.
[11] M. Cacciari, G. P. Salam, G. Soyez, FastJet User Manual, Eur.Phys.J. C72 (2012) 1896. arXiv:1111.6097, doi:10.1140/epjc/s10052-012-1896-2.
[12] P. Berta, M. Spousta, D. W. Miller, R. Leitner, Particle-level pileup subtraction for jets and jet shapes, JHEP 06 (2014) 092. arXiv:1403.3108, doi:10.1007/JHEP06(2014)092.
[13] H.A.Andrews, Studies of jet grooming and recursive splittings in pp and Pb–Pb collisions with ALICE, Quark Matter 2018 (2018).
     URL https://indico.cern.ch/event/656452/contributions/2869941/